SPE 113864

Pore-Scale Simulation of WAG Floods in Mixed-Wet Micromodels

M.I.J. van Dijke, M. Lorentzen, SPE, M. Sohrabi, SPE, and K.S. Sorbie, SPE, Heriot-Watt U.

This paper was prepared for presentation at the 2008 SPE/DOE Improved Oil Recovery Symposium held in Tulsa, Oklahoma, U.S.A., 19–23 April 2008.

Abstract

In this paper the simulation is described of water-alternating-gas injection (WAG) flood cycles in 2-D etched glass mixed-wet micromodels, using a 3-D pore-scale network model for three-phase immiscible flow in porous media of arbitrary wettability. Although most network model input parameters can be explicitly derived from the experiments, the precise wettability parameters are not directly available. Therefore, a sensitivity study was carried out, using the network model in 2-D mode, to obtain the wettability characteristics, i.e. the contact angle values and distribution, and the fraction of water-wet pores. Good qualitative and quantitative agreement was found between the experimental and simulated recoveries over the various WAG cycles, and the final residuals were well reproduced (as well as some observed "random recovery jumps"). The simulated displacement statistics showed many so-called multiple displacement chains involving oil, up to around the third WAG cycle. The experimental and simulated fluid distributions were generally in good agreement in that (a) different gas fingers were observed during various gas floods, (b) oil movement was observed mainly during the first few WAG cycles, and (c) during water floods, significant amounts of gas were displaced. Additionally, previously described simulations of water-wet and oil-wet experiments are compared with the present mixed-wet simulations. There are close similarities between the mixed-wet and oil-wet cases, which both maintain some continuity of oil through wetting films, but these cases are quite different from the water-wet case, which has continuity of water through wetting films in all pores. This paper further validates the pore-scale mechanisms incorporated in a network model that is capable of predicting three-phase relative permeabilities and capillary pressures for complicated processes such as WAG.

Introduction

Modelling hydrocarbon recovery processes involving three-phase flow, such as Water-Alternating-Gas injection (WAG) requires accurate knowledge of the corresponding capillary pressure and relative permeability functions. However, there are significant experimental difficulties in obtaining these quantities and over recent years pore-scale network models are emerging as potential predictive tools. These models take into account the pore-scale flow mechanisms, which in turn have to be underpinned by observations from microscopic flow experiments. Micromodels consisting of a 2-D porous structure etched in glass or other transparent materials are of great help in visualising these mechanisms. When the detailed flow mechanisms are incorporated in the network model, we may then directly compare the network flow simulations with the micromodel flow experiments, as a way of validating the network model (e.g. van Dijke *et al.*, 2004, 2006). In the present paper, this task has been carried out for WAG experiments in mixed-wet micromodels, described by Sohrabi *et al.* (2001, 2004).

Several authors have emphasised the importance of the spreading behaviour (of oil) on the pore-scale three-phase flow mechanisms, as well as the role of the wettability of the medium (see e.g. Øren and Pinczewski (1995), Vizika and Lombard (1996), Keller *et al.* (1997) and Dong *et al.* (2005)). In strongly water-wet media, the presence or absence of spreading oil layers in gas filled pores plays an important role in improving oil recovery. In oil-wet and weakly water-wet media it is the presence or absence of oil wetting films surrounding the water and gas phases, depending on the degree of wettability, that may enhance recovery. This affects the detailed mechanism of which phase displaces which and in what size of pore (van Dijke and Sorbie, 2002b).

Three-phase flow experiments in oil-wet micromodels have been described by Øren and Pinczewski (1994) and Laroche (1998) involving immiscible gas flooding. Based on such micromodel experiments, Øren and Pinczewski (1995) have described all pore-scale fluid configurations and flow mechanisms in oil-wet systems for both spreading and non-spreading oils. Additionally, the experiments of Øren and Pinczewski (1994) and Laroche (1998) have been reproduced using network models by Pereira (1999) and Laroche *et al.* (1999), respectively. Pereira described the qualitative features of the simulated gas injection in water flood residual oil, which agree well with the experimental observations. These features include a high

frequency of double gas-water-oil displacements (g→w→o) and the tendency of gas to displace complete isolated oil clusters, as soon as gas touches these clusters, for both the spreading and the non-spreading oil in the oil-wet system. Notice that this phenomenon is a direct consequence of the presence of oil wetting films around water, which facilitate escape of oil to the outlet. Moreover, Pereira found very good quantitative agreement between simulation and experiment for the (large) volumes of oil and water recovered at the end of the gas flood. For gas injection at irreducible water saturation in the uniformly oil-wet micromodel Laroche *et al.* (1999) found high recovery, which they attributed to blocking of the large pores by water, leading to high sweep efficiency. However, they obtained poor quantitative agreement between simulation and experiment, which was attributed to finite size effects.

Only more recent experimental and modelling work has examined the fluid displacement patterns and the oil recovery in higher WAG cycles. Van Dijke *et al.* (2004) have directly compared WAG experiments in a strongly water-wet micromodel (Sohrabi *et al.*, 2004) with simulations in a corresponding 2-D network model using the same experimental parameters. In agreement with experimental observations spreading layers of oil around gas were suppressed in the modeling. The central conclusion of this comparison was that the network model reproduced the qualitative behaviour in the later WAG cycles very well: the gas clusters were broken up and oil and gas were redistributed in the network leading to small (and decreasing) amounts of additional oil recovery. The comparison focussed in detail on the three-phase fluid distributions, the oil recoveries after the various floods and the displacement statistics. The latter consists of histograms of the lengths of the so-called (multiple) displacement chains and the involved types of displacements. Dong *et al.* (2005) also analysed WAG experiments in a water-wet micromodel with a profoundly spreading oil. They emphasized that the (strongly declining) oil recovery throughout the WAG cycles occurred mainly as a result of water displacing oil that had been pushed by the gas floods into previously established water channels.

Furthermore, van Dijke *et al.* (2006) have directly compared WAG experiments in an oil-wet micromodel (Sohrabi *et al.*, 2004), where oil wetting films around water were important. The central observation in the oil-wet experiment and modeling that the gas clusters were broken up and oil and gas were redistributed in the model was similar to that for the water-wet case. However, in the oil-wet model oil production ceased after fewer WAG cycles. A more detailed comparision of the various experiments and simulations is presented later in this paper. Suicmez *et al.* (2007) have carried out a network modeling study of WAG, which focused on the prediction of displacement paths and relative permeabilities from core flood experiments in both water-wet and oil-wet media.

In this paper, we compare simulation results from the same network model as used for the water-wet and oil-wet systems with WAG experiments in a mixed-wet micromodel (Sohrabi *et al.*, 2001, 2004), i.e. having fractions of both (weakly) water-wet and oil-wet pores. The 3-D network model, which is used here in 2-D mode, has extensively been described before (van Dijke and Sorbie, 2002a, 2003; van Dijke *et al.*, 2004, 2006). Three micromodel experiments were carried out, for slightly different wettability conditions each. First, we briefly describe the experiments and the network model set-up. Because some uncertainty exists regarding the (wettability) input parameters for the simulations, a limited sensitivity study has been carried out with respect to these parameters against the experimental residual oil saturations during the consecutive WAG floods, which leads to a base case simulation that matches the experimental recovery trend. For this simulation also the displacement statistics are presented. Then, the detailed simulated and experimental fluid distributions for each WAG flood are compared. Finally, a comparison is made between the current modelling of mixed-wet experiments and previous simulations of water-wet and oil-wet experiments (van Dijke *et al.*, 2004, 2006)

Using the network model in the described manner to directly simulate the 2-D micromodel experiments is not strictly predictive. Instead, it is using the model as a validation of the assumptions on the underlying pore-scale mechanisms (on films and wettability). However, once this has been done, the (3-D) network model may then be used to predict emergent three-phase relative permeabilities and capillary pressures at the macroscopic scale for these assumptions concerning the behaviour of films and the wettability.

Experiment description and network model set-up

Experiments

Sohrabi *et al.* (2001, 2004) have reported WAG micromodel experiments for three mixed-wet systems starting with a water flood into an oil saturated model, followed by WAG injection cycles (five cycles of gas injection followed by water injection). The vertically positioned acid-etched glass micromodel has 120 × 20 nodes, connected by rectangular pores, with co-ordination number $z = 2.67$. Pore widths are distributed randomly, ranging from about 90 to 280 μm and the depth of the pores is roughly a constant 50 μm. The length of the pores is 350 μm. The water, oil (n-decane) and gas (methane) densities are ρ_w =1000 kg/m^3, ρ_o = 706 kg/m^3, ρ_g = 21 kg/m^3, respectively. Interfacial tensions (IFTs) have been reported as σ_{gw} = 65 mN/m, σ_{go} = 15 mN/m and σ_{ow} = 41 mN/m.

Initially, the micromodel was completely rendered oil-wet by ageing with a North Sea crude oil and then brought back to mixed-wet conditions after continous injection of dyed water Sohrabi *et al.* (2001, 2004). Using this approach, three different mixed-wet conditions were established, for which the contact angle θ_{ow} of the oil-water interfaces (around 1000 in the whole micromodel) after the water injection were examined. The interfaces were classified as water-wet $\theta_{ow} < 85^o$, neutral-wet

$85^o < \theta_{ow} < 95^o$ or oil-wet $\theta_{ow} > 95^o$, as shown in Table 1, while very few pores were strongly wetted (θ_{ow} close to 0 or 180 degrees).

Table 1- Wettability conditions used for the reported mixed-wet experiments. Percentage of oil-water interfaces for each wettability type (Sohrabi *et al.*, 2004).

Experiment No.	% Water-wet	% Oil-wet	%Neutral-wet
1	36.4	46.7	16.9
2	43.2	35.2	21.6
3	38.3	37.9	23.8

After ageing, the model was filled with water and subsequent oil and water floods were performed, followed by a number of gas and water floods (WAG cycles). All floods in were carried out at a rate of 0.01 cm^3/h, except for the initial oil flood, which was performed at a rate of 2 cm^3/h to establish the desired initial oil saturation. Further experimental details have been provided by Sohrabi *et al.* (2001, 2004). In Figure 1 the residual oil saturations after each WAG flood for the three micromodels are presented.

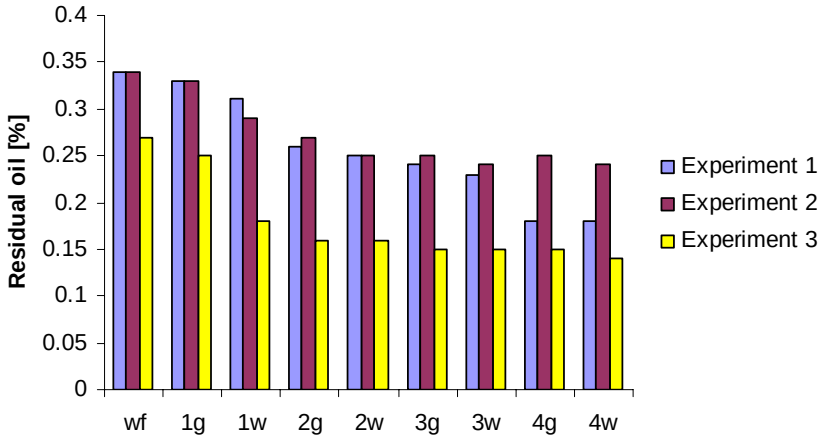

Figure 1 – Residual oil saturations during the various experiments. wf indicates initial two-phase water flood and, for example, 3g denotes gas flood in third WAG cycle.

Network model set-up

Network simulations have been performed to match the WAG floods in the micromodel. We have simulated a network with a geometry that is statistically similar to the micromodel, with similar pore size distributions and co-ordination number. For each flood the inlet is at the bottom of the model, where the pressure of the invading phase is imposed. The outlet is at the top of the model where the pressures of the three phases are fixed, although it has been shown that gravity has a negligible effect on flow. The lateral boundaries have no-flow conditions for each of the three phases. Arbitrary wettability states can be assigned, as well as films of the wetting phases and oil spreading layers, guided by the wettability conditions. The wettability, film and layer parameters are specified in the next section. The length of multiple displacement chains is restricted to 5. Detailed descriptions of the capillary dominated invasion-percolation network model have been given by van Dijke and Sorbie (2002a, 2003) and van Dijke *et al.* (2004, 2006).

The simulation starts with a totally water filled model, which is flooded by oil to the maximum attainable saturation (0.43), which is significantly less than in the experimental data (0.65), probably due to the higher flow rate in the latter. After the initial oil flood, an initial water flood was simulated followed by four WAG cycles, each run until breakthrough. Simulation results have been compared with the experiments based on different characteristics such as fluid distributions after the various floods, displacement type statistics and recovery profiles.

Determining the wettability input parameters for the network simulations

In Table 1 the three mixed-wet experiments have been classified as “more oil-wet” (experiment 1), “more water-wet” (experiment 2) and “neutral wet” (experiment 3) and it has been noted that most pores were weakly wetted by either oil or water. However, no link between contact angles and pore sizes was provided. In other words, it cannot be determined whether the micromodel is mixed-wet with the smaller or the large pores oil-wet (MWS or MWL). For this reason, in the simulations we assume a fractionally (FW) wet model where a random fraction of pores of any size may be oil-wet. Determination of the fraction of water-wet and oil-wet pores is part of a small sensitivity study, presented below, as are the actual values of the oil-water contact angles.

Because almost all pores are weakly wetted (either water-wet or oil-wet) no water wetting films or oil wetting films around water were apparent. Although the oil spreading coefficient $C_{S,o} = \sigma_{gw} - \sigma_{go} - \sigma_{ow}$ was equal to zero, there was little evidence in the experiments of oil spreading layers or oil wetting films around gas in oil-wet pores. Notice, that spreading layers were also *not* observed in the water-wet experiments (Sohrabi *et al.*, 2000, van Dijke *et al.*, 2004). It is well known that the presence of oil wetting films or spreading layers has a profound impact on the recovery profile. For weakly wetted pores, both water-wet and oil-wet, it is most likely that oil wetting films around bulk gas are more likely than oil spreading layers or indeed oil wetting films around water (van Dijke *et al.*, 2004). Therefore, we also consider the presence and absence of this wetting films in our sensitivity study.

The sensitivity study is carried out against the residual oil saturations for the three micromodel experiments, as presented in Figure 1. The general conclusion might be that most recovery takes place during the first two WAG cycles, but otherwise these production data appear quite different for the three experiments, containing significant "random" variation , which may or may not have been caused by experimental error. For example, after the fourth gas flood (4g) of experiment 1 and after the first water flood (1w) of experiment 3 (1w) "random" jumps in production occur, whereas after the fourth gas flood of experiment 2 the oil saturation increases. Also, the big difference in residual oil after the initial water flood between experiment 15 and the other two experiments seems "random". This makes it difficult to draw strong conclusions about the recovery trends and to distinguish the experiments, hence choosing the precise input for simulating the individual experiments is not obvious.

Based on the sensitivity study we choose one simulation, which reasonably matches both the wettability input and the experimental production data for the three experiments together. For this simulation we compare in detail the fluid distributions and displacement mechanisms with those for one of the experiments.

Sensitivity study with respect to wettability parameters

In Table 2 nine different cases for the wettability parameters are listed, which are all broadly consistent with the experimental input as far as we know them. Wetting films and spreading layers were suppressed, except oil wetting films around gas. The effect of suppressing also the latter is studied in case 7a.

Table 2– Wettability parameters for the different cases in the sensitivity study. For cases 1 to 6 the first value applies to the constant (oil-water) contact angle in the water-wet pores and the second value applies to the oil-wet pores. For cases 7, 7a and 8 a uniform distribution of contact angles in the indicated ranges is chosen.

Case	Fw*	Contact angles (degrees)	Constant/Distributed angles
1	0.5	60,120	Constant
2	0.3	60,120	Constant
3	0.7	60,120	Constant
4	0.5	75,105	Constant
5	0.3	75,105	Constant
6	0.7	75,105	Constant
7	0.5	60-120	Distributed
7a**	0.5	60-120	Distributed
8	0.5	75-105	Distributed

***** Fw denotes fraction of water-wet pores

** In case 7a oil wetting films around gas were suppressed, contrary to the other cases

The results of the sensitivity study are presented in Figure 2 in groups of cases where only one of the parameters is varied. In the first three cases from Table 2 only the fraction of water-wet pores is varied. For case 2 no oil is produced after the first WAG water flood whereas residuals for case 3 are consistently higher than for the other cases. As in the experiments, "random" jumps in residual oil appear, which makes it difficult to distinguish between cases 1 and 2, and both may be in agreement with the experimental observations presented in Figure 1. However, quantitatively the residuals of these simulations agree very well with the experimental results.

For cases 4 to 6 also the fraction of water-wet pores is varied, but the contact angles are different from those of cases 1 to 3. The qualitative difference between cases 1 to 3 and 4 to 6 is that in the latter water is wetting to gas in the oil-wet pores (van Dijke and Sorbie, 2002b). The more oil-wet case 5 has the lowest residuals and the more water-wet case 6 has the highest residuals. Interestingly, the residuals for the three cases are further apart for cases 4 to 6 than for cases 1 to 3, although the averages are roughly the same, and also the intermediate cases with equal numbers of water-wet and oil-wet pores (cases 1 and 4) are very similar. However, this seems to contradict the trend in the experimental results shown in Figure 4.2 where experiment 3 with roughly equal fractions of water-wet and oil-wet pores leads to the lowest residuals.

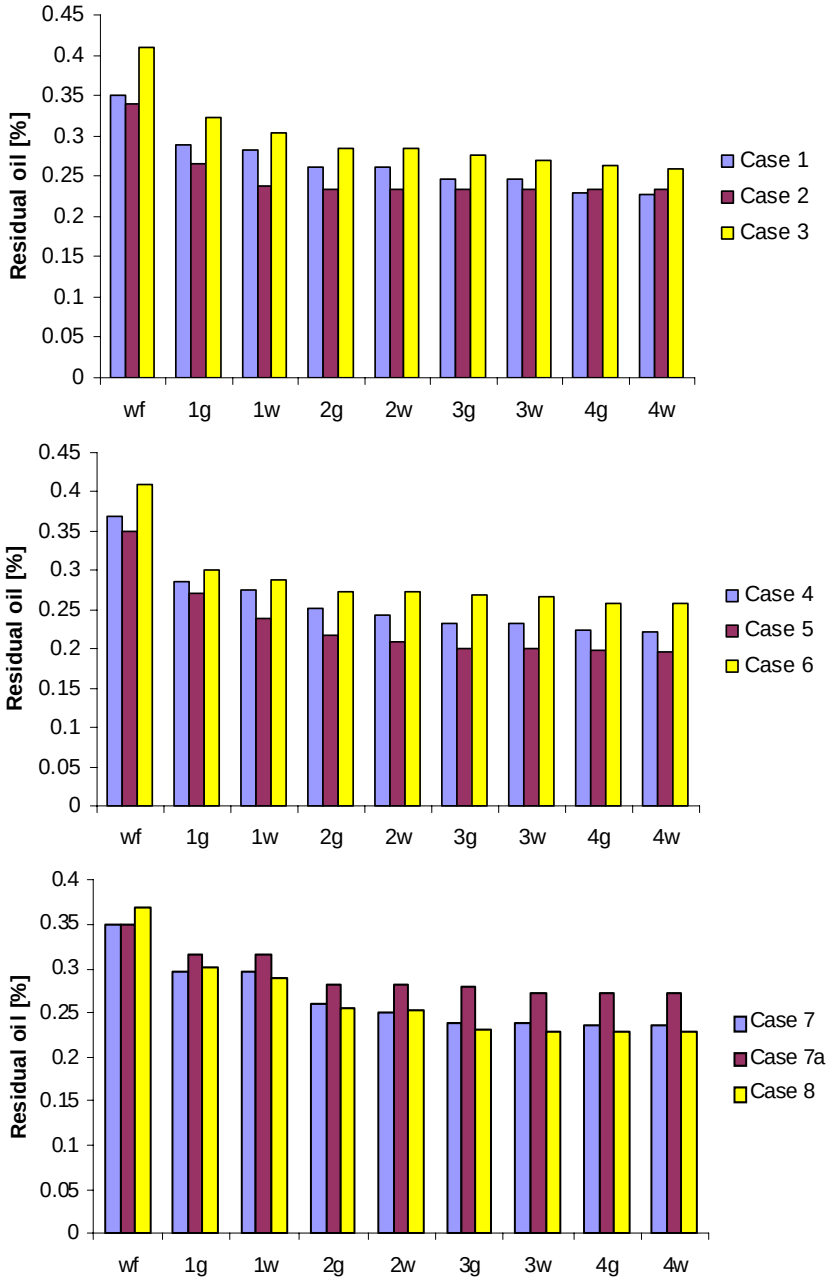

Figure 2 – Residual oil saturations during the simulations with parameters listed in Table 1.

For cases 7, 7a and 8 the contact angles are uniformly distributed over two different ranges, with equal fractions of water-wet and oil-wet pores. The residual oil saturations for cases 7 and 8 are very similar and they are also almost identical to those for the corresponding constant contact angle cases 1 and 4. In other words, at least for the cases with equal fractions of water-wet and oil-wet pores, the fact that the contact angle values are distributed, rather than constant, seems to have little effect. Suppressing oil wetting films around gas as in case 7a leads to consistently higher oil residuals, as we would expect.

Comparing the experimental residual oil saturations of Figure 1 with the simulated residuals of Figure 2 shows that it is difficult to choose a "best" case from the simulations. Quantitatively, the final residuals of most simulations are closest to those of experiment 2 (around 23%). The only real discrepancy between the experimental and simulation results seem to appear during gas flood 1, where all simulations indicate a significant drop in residual oil, contrary to the experiments, although case 7a performs slightly better in this respect. However, during the later WAG cycles these differences level out for most cases.

Considering that it is difficult to choose between the "asymmetric" cases with either more water-wet or more oil-wet pores, since the trends in the simulated and experimental residuals seem to contradict each other, and because the measured contact angles had a certain distribution range, we select case 7, called the base case, as the simulation for which results will be compared directly with the experiments. From experimental observations, there is little evidence of oil wetting films around

gas. However, recoveries without this feature are too small, as shown for case 7a. Therefore, since it is in line with the spreading nature of the oil, oil wetting films around gas are not suppressed.

In Figure 3 the experimental residuals and additional recoveries of water flood residual oil are compared with those for case 7. There is good agreement of experiments 1 and 2 with case 7 for WAG cycles 1, 2 and 3, before the "random" drop in the residual oil during the fourth gas flood in experiment 1. The recovery profile shows that case 7 also approximates the experimental recoveries well, when the effect of differences in initial oil saturations is taken away. In the next section, we will compare in more detail case 7 and experiment 2, since their recoveries match best.

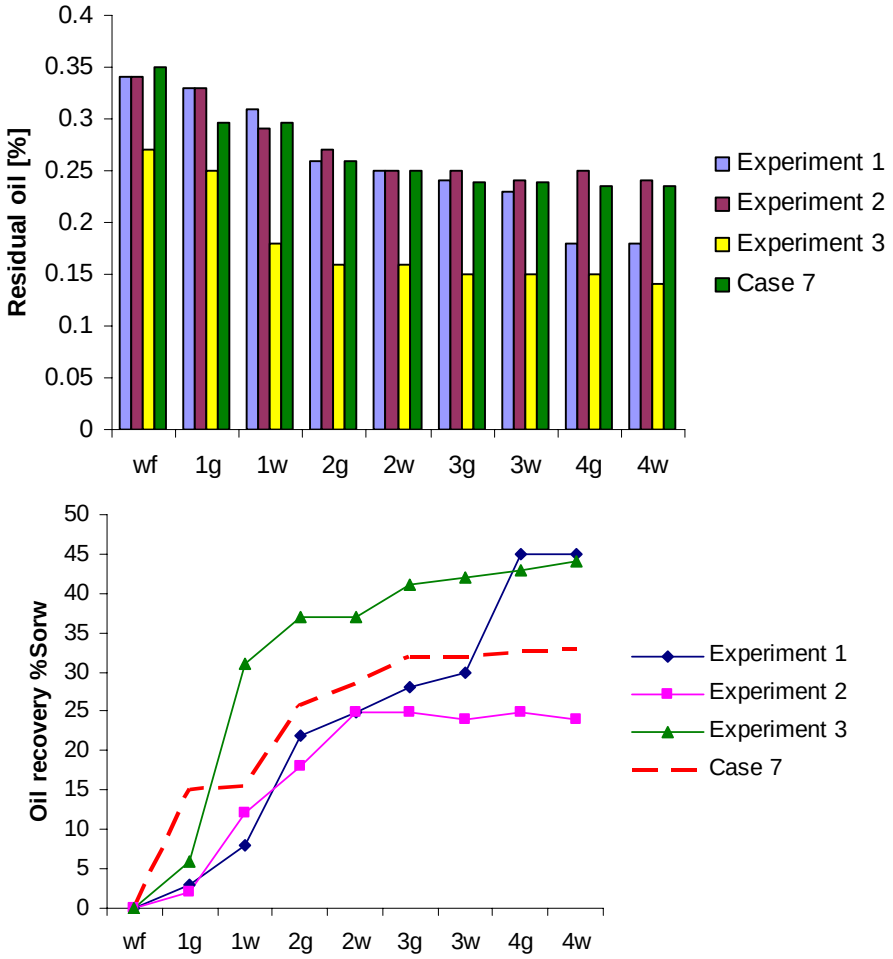

Figure 3 – Residual oil saturations and additional oil recovery during WAG for the base case simulation (case 7) compared to the three experiments.

Comparison of fluid distributions for the base case simulation and the experiments including displacement statistics

Based on the sensitivity study with respect to the wettability parameters in the previous section, the simulation of the base case (case 7 in Table 1) has been selected for comparison with the experiments, in particular experiment 2. The simulated fluid distributions of the base case are compared directly with the fluid distributions observed in the experiment, and also the displacement statistics, predicted by the simulation, are analysed. In the snapshots of the fluid distributions only half the micromodel is shown, corresponding to a 20x60 network model.

Additional information about the precise displacements during the simulation is presented in Figure 4, which shows the fraction of the different types of displacements during each flood, as well as the fraction of displacement chains with the indicated lengths (van Dijke and Sorbie, 2003). For example, a displacement chain involving gas (at the inlet), displacing water, displacing oil, displacing gas (at the outlet), is a displacement chain of length 3 containing the individual displacements g→w, w→o and o→g. It is clear that many multiple displacement chains occur, up to the third WAG cycle, with many displacements involving oil (noticeably o→g and o→w). This means that during these floods many disconnected phase clusters, in particular oil clusters, are moved within the network. The last three floods are dominated by w→g and g→w displacements, not involving oil. The fraction of single displacements increases for every flood after the second gasflood, while the last flood consists almost exclusively of single displacements (indeed w→g or g→w). This is consistent with the observation from Figure 3 that hardly any oil is produced during the last three floods.

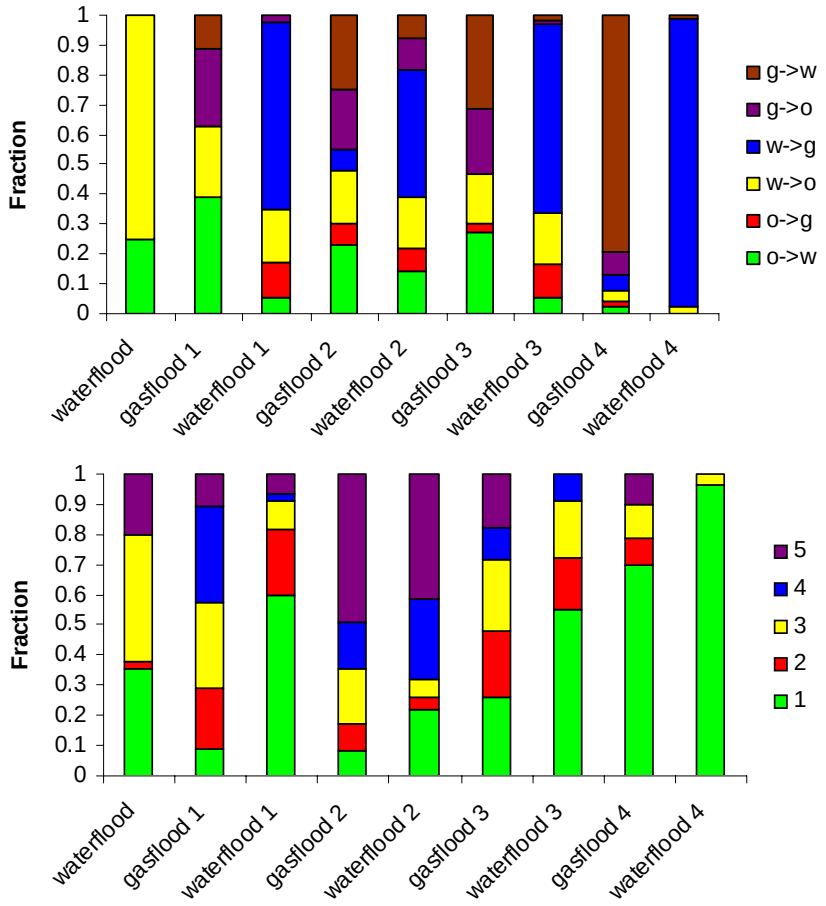

Figure 4 - Types of displacement and displacement chain lengths during consecutive WAG cycles for the base case simulation. Displacement type records the frequency of each displacement (as part of a displacement chain) during a given flood. Chain length records the frequency of (multiple) displacement chains of the indicated lengths.

In Figure 5 the simulated and experimental fluid distributions after the initial oil and water floods are presented. Because of the higher oil injection rate in the experiment, more oil filled pores can be observed in the experiment than in the simulation after the oil flood. The snapshots after the initial water flood reveal that there are trapped oil clusters in both the simulation and the experiment, as water has broken up the oil flow paths in both networks. Consistent with Figure 3, we find that the amounts of residual oil are very similar in simulation and experiment. Figure 4 shows that already during the simulation of this (higher order) two-phase flood multiple displacement chains occur, that a substantial 25% of the displacements are o→w (oil displacing water). In a capillary dominated two-phase flood displacement chains can only occur if a disconnected phase cluster is surrounded by separate clusters of the other phase. In most situations, this is very unlikely, but in the current 2D network with a width of only 20 pores and low connectivity, this is possible. It is difficult to confirm that these displacement chains also occured during the experiments.

From the snapshots after the first gas flood, presented in Figure 6, a narrow gas finger can be seen in both simulation and experiment. Even though it is slightly wider in the simulation, the qualitative behaviour is the same. The wider gas finger may be the reason why the oil residual in the simulation is lower in the simulation than in the experiment, shown in Figure 3. The gas finger displaces both oil and water, and there is evidence that oil has been pushed into water through double and multiple displacements. This is confirmed by Figure 4, where we find all kind of displacements during this gas flood, from single up to 5 displacements, with many w→o and o→w displacements.

During the first WAG water flood, some differences are observed between simulation and experiment. In the simulation, gas is not dispersed as much as it is in the experiment, but rather water displaces gas, which can also be seen from Figure 4. In the experiment it is observed that water breaks up the gas clusters and pushes gas into oil. The latter may cause more multiple displacement chains then recorded for the simulation in Figure 4. Observe from this figure that the simulated water flood 1 may be a “random” exception with relatively few multiple displacements, in comparison in particular the second water flood. This probably explains also the lack of oil production, apparent from Figure 3, contrary to the experiment.

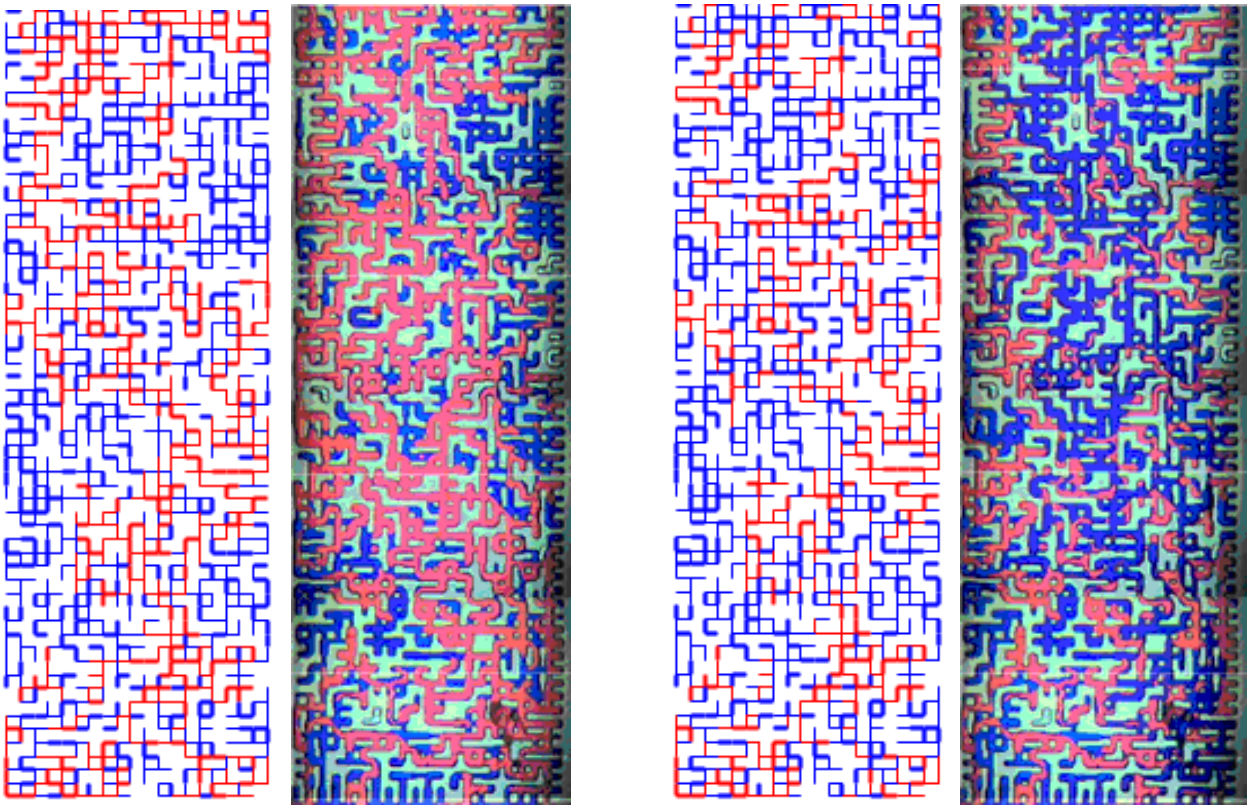

Figure 5 – Fluid distributions in the network model (left) and micromodel (right) after the initial oil and water floods. Blue water, red oil.

The fluid distributions after the second gas flood, presented in Figure 7, reveal that gas takes a different path compared to the first gas flood. This happens in both simulation and experiment, resulting in many multiple displacements according to Figure 4, as well as additional oil production, as seen from Figure 3. Significant numbers of every type of displacement occur.

Comparison of the second gas and water flood distributions shows that during the second water flood, oil movement in the experiment slightly exceeds the simulated oil movement. This is consistent with the recovery profile of Figure 3, which shows more oil recovery in the experiment than in the simulation. However, the main feature in both simulation and experiment is that a significant amount of gas is displaced and that the remaining gas has roughly the same configuration. Figure 4 confirms the displacement of gas, as around 40% w→g displacements occur.

In the simulated fluid distributions after the third gas flood, shown in Figure 8, a new gas finger arises at the top of the model. During this flood a certain amount of water is displaced by gas in both simulation and experiment, while in the simulation an additional 2-3% oil is produced compared to the second waterflood, according to Figure 3. Furthermore, in the simulation some oil is redistributed within the model, which is also evident from the displacement statistics, but in contrast to the experimental observations.

As observed earlier, from the second water flood onwards hardly any additional oil is produced and the number of multiple displacements decreases. The displacement statistics of Figure 4 confirms that mostly exchanges of water and gas occur, as demonstrated by the fluid distributions in Figures 8 and 9. For example, widening of the gas finger after the fourth gas flood, as shown in Figure 9, happens mostly at the expense of water, although in the experiment still some redistribution of oil can be observed.

In general, very good agreement is found between the base case simulation and experiment 2, even on the level of the fluid distributions. Although during most floods in the experiment redistribution of oil is more noticeable than in the simulation, also in the simulation redistribution is clearly seen during the second gas and water floods. For the second gas flood this has led to a significant additional oil recovery in both simulation and experiment. In the later WAG floods the oil production ceases and mostly exchanges of water and gas occur. These observations are confirmed by the simulated saturation path shown in Figure 10 and by the displacement statistics of Figure 4.

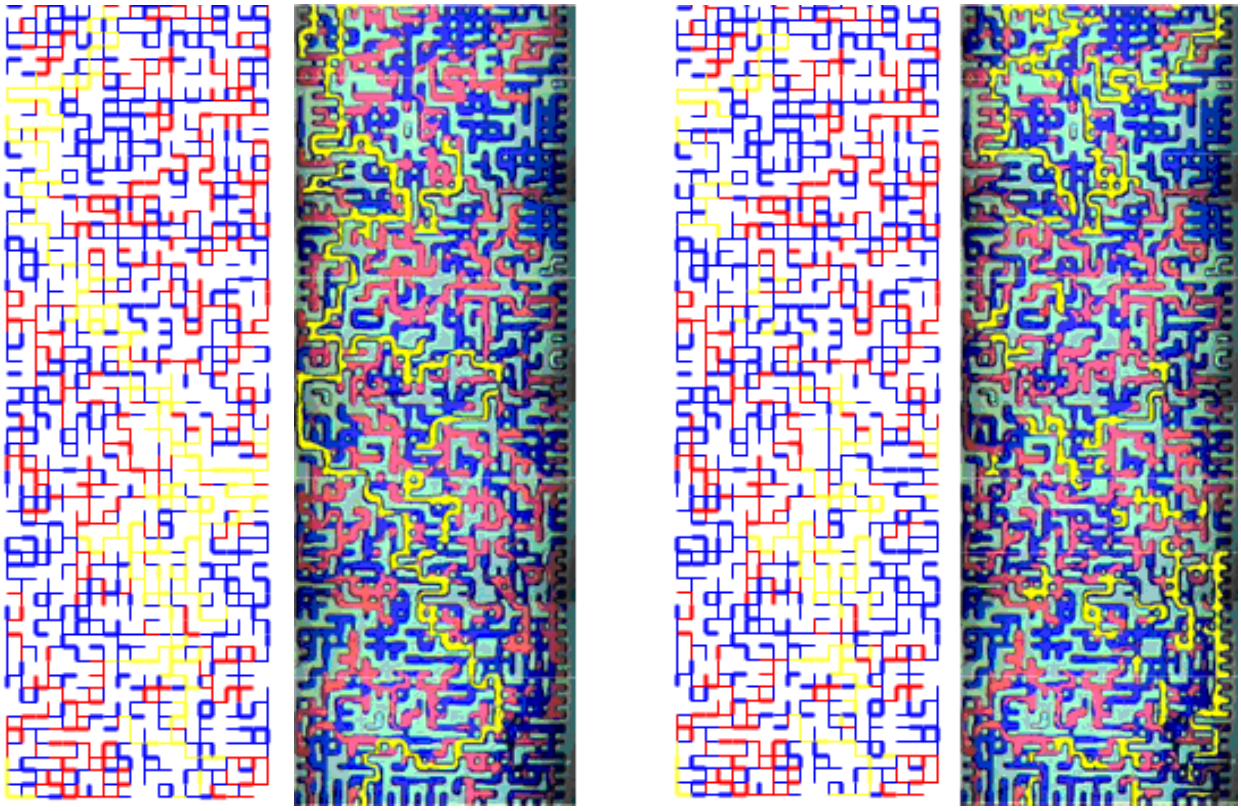

Figure 6 - Fluid distributions in the network model (left) and micromodel (right) after the first gas and water floods. Blue water, red oil, yellow gas.

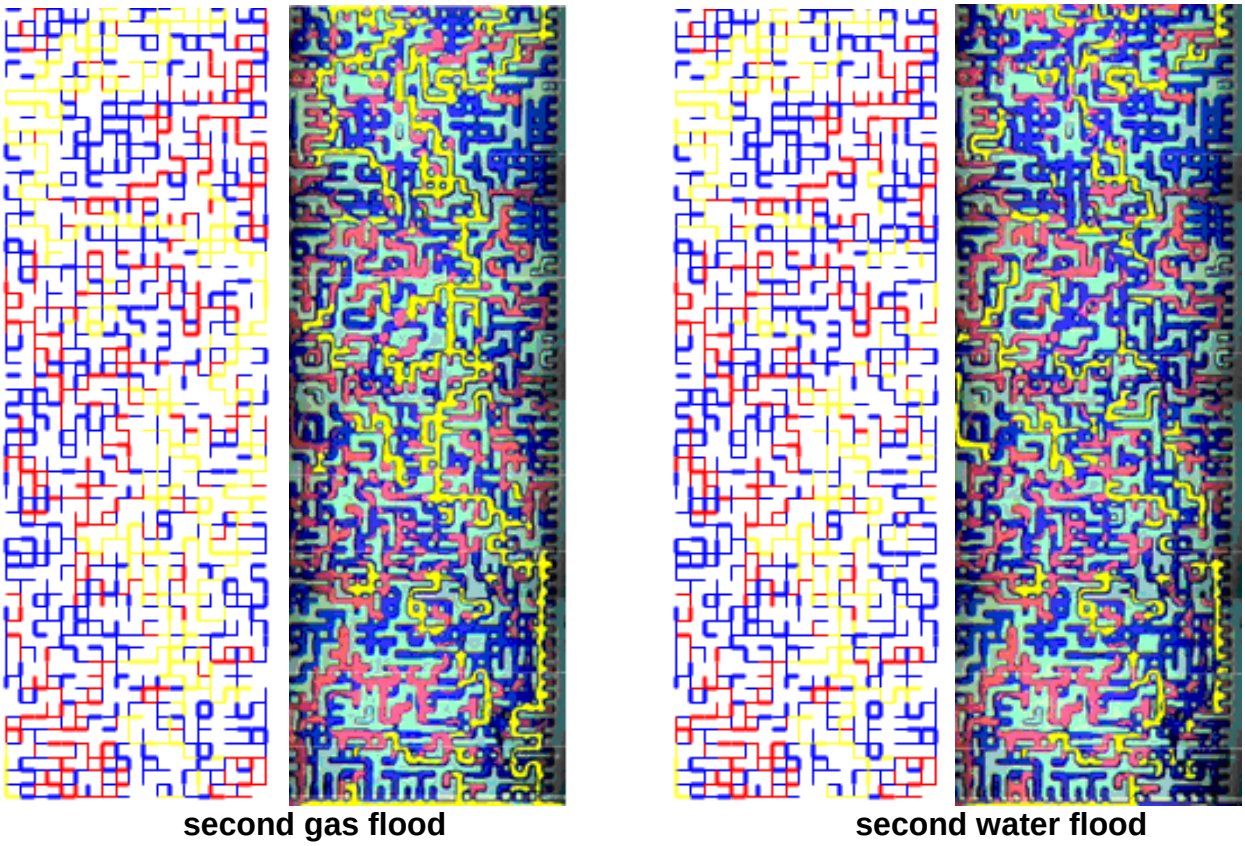

Figure 7 - Fluid distributions in the network model (left) and micromodel (right) after the second gas and water floods.

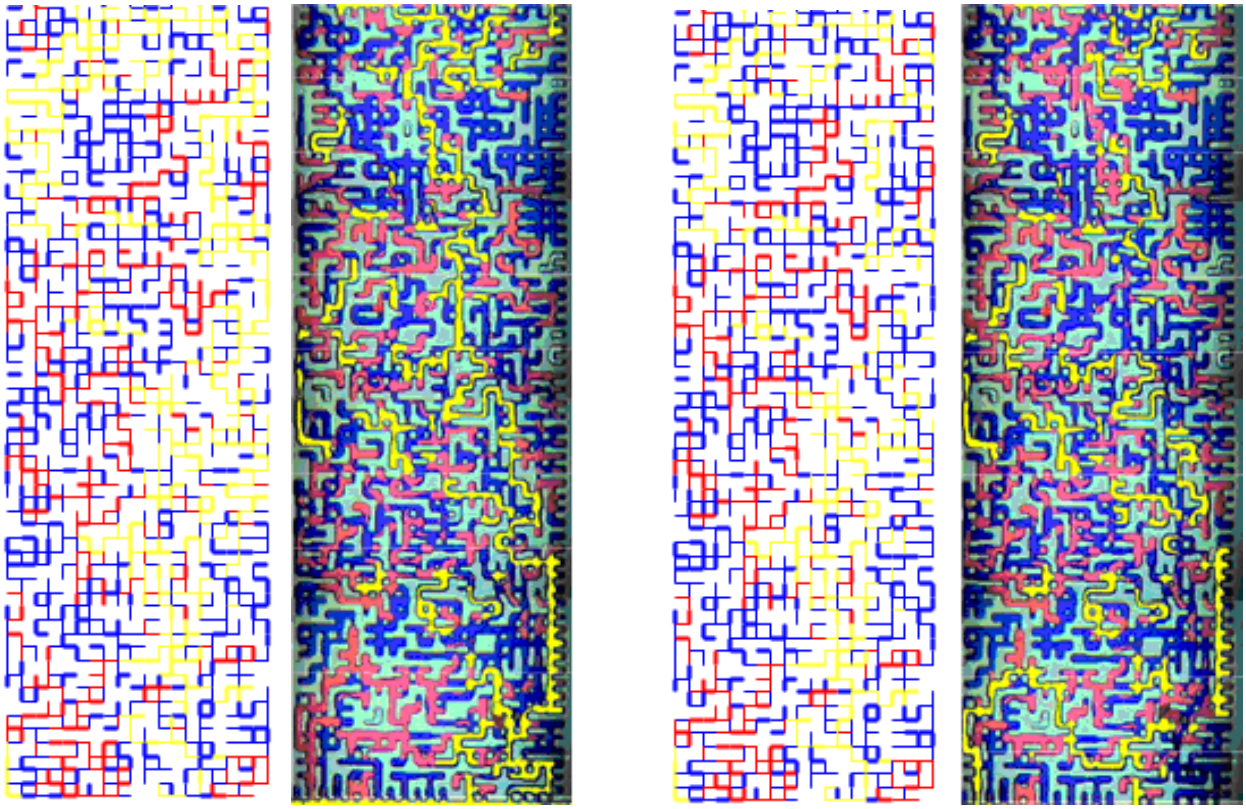

Figure 8 - Fluid distributions in the network model (left) and micromodel (right) after the third gas and water floods.

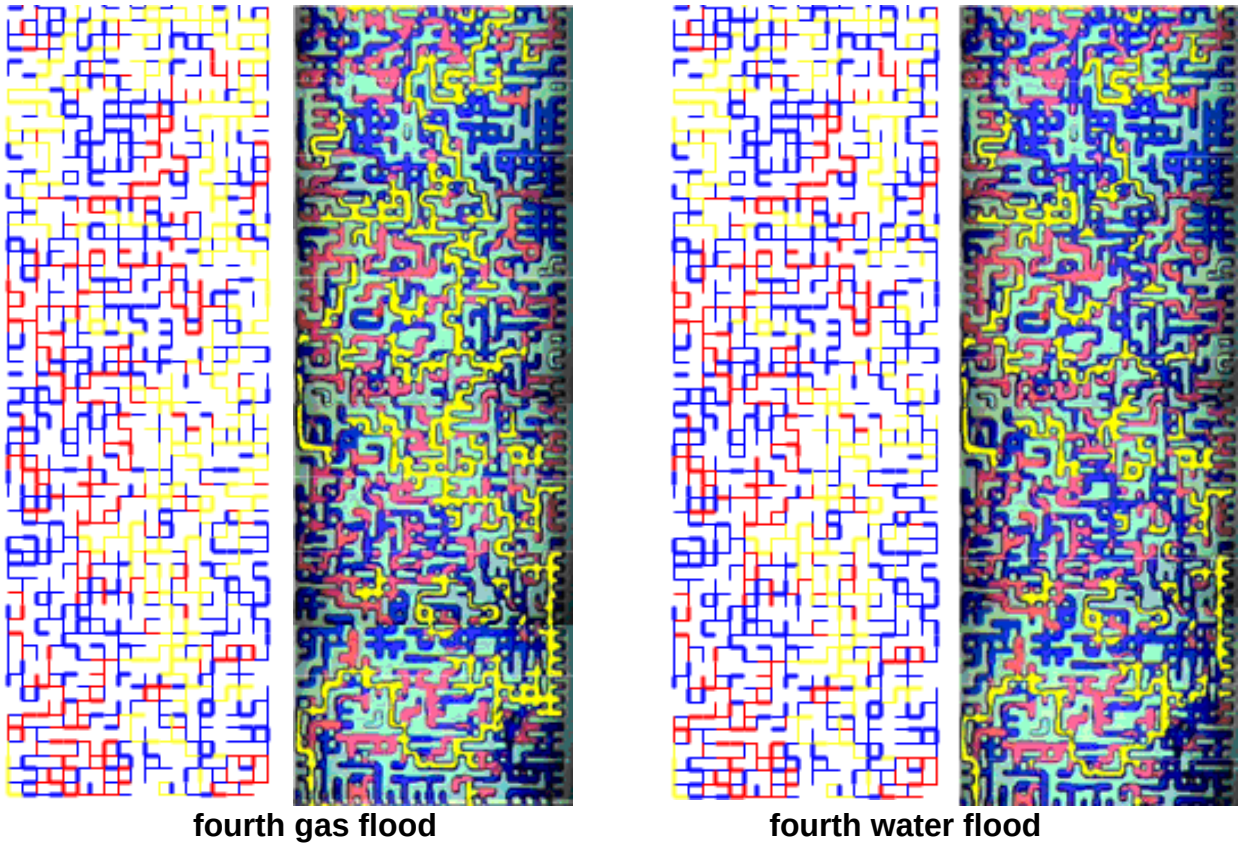

Figure 9 - Fluid distributions in the network model (left) and micromodel (right) after the fourth gas and water floods.

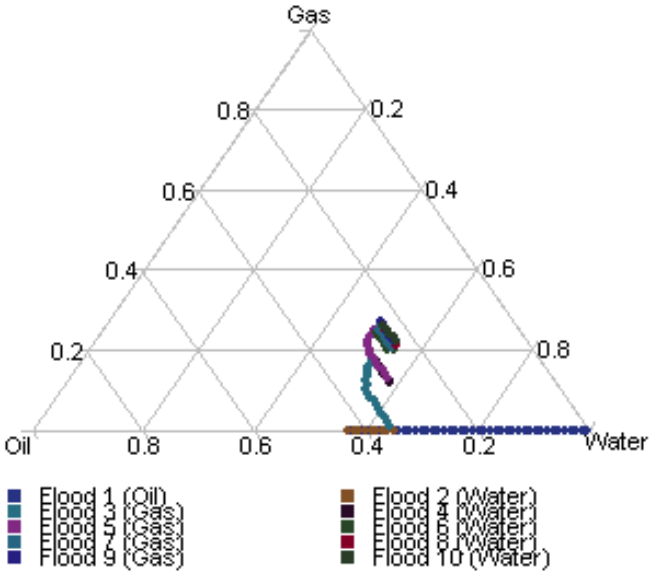

Figure 10 - Saturation path for the base case WAG simulation.

Comparison of the simulations of the water-wet, oil-wet and mixed-wet experiments

In this section, the simulations and experiments described above will be discussed in the light of the simulations used for comparison with the water-wet (van Dijke *et al.*, 2004) and oil-wet (van Dijke *et al.*, 2006) micromodel experiments. The simulated residual oil saturations and displacement chain statistics will be compared.

The main difference between the simulations of the three sets of experiments is obviously in the values used for the contact angles and the corresponding presence or absence of films and layers. In the water-wet model (van Dijke *et al.*, 2004), $\cos\theta_{ow} = 1$ was used uniformly and water wetting films were present. The interfacial tensions were the same as for the present mixed-wet model, yielding a spreading oil. However, similar to the base case simulation above, spreading oil layers were suppressed. The simulations started with primary drainage followed by an initial water flood. Then, a series of WAG cycles of gas followed by water were simulated.

For the oil-wet micromodel the precise contact angle values were unknown and a sensitivity study was carried out, similar to that for the present comparison with the mixed-wet experiments, to find a reasonable input for the wettability (van Dijke *et al.*, 2006). A good match with the experimental observations was obtained by choosing strongly oil-wet conditions, i.e. $\cos\theta_{ow} = -1$ uniformly, but oil wetting films around water were allowed in only 33% of the pores, while oil wetting films around gas were suppressed. However, the observed residuals could also reasonably be matched by allowing some oil wetting films around gas rather than around water. Obviously, in the present mixed-wet simulations only oil wetting films around gas have been allowed, as oil wetting films around water contradict the weakly wetted nature of the oil-wet pores.

Below, we only consider the simulation starting with an initial water flood in 100% oil, as opposed to the simulation starting with an initial gas flood. After the initial water flood a series of WAG cycles of gas followed by water were simulated.

Comparison of the residual oil saturations

In Figure 11 the residual oil saturations resulting from simulation of the water-wet and oil-wet experiments are presented. Compared to the residual oil saturations for the current mixed-wet experiments, presented in Figure 3, seems to indicate that the water-wet case was much less efficient. This difference originates from very different initial water floods. In the water-wet experiments the water flood was carried out in around 70% oil saturation and little recovery occurred during this flood, around 3%. This lack of recovery is not in agreement with the experiment and this issue has been discussed in detail before (van Dijke *et al.*, 2004). On the other hand, in the mixed-wet case the water flood was carried out in 43% oil saturation of which around 8% was recovered, showing good agreement with the experiment. The oil-wet model had a residual oil saturation of 51% after the initial waterflood, which is 16% more than in the mixed-wet case. However, this is mainly the result of the different initial conditions, as the water flood for the oil-wet case was carried out in a fully oil saturated model.

Both the water-wet and the mixed-wet simulations show a significant recovery during the first gas flood, although the recovery in the corresponding experimental gas floods was less. During the consecutive WAG floods, both simulations show a gradual decline of the residual oil saturations with some “random” jumps, as for example after the second and fourth gas floods in the water-wet case (Figure 11), in agreement with the “random” jumps observed during the experiments. Also for the oil-wet case, the first gas flood resulted in a significant recovery, but this is much more in agreement with the experiment and it is probably the result of the presence of oil wetting films.

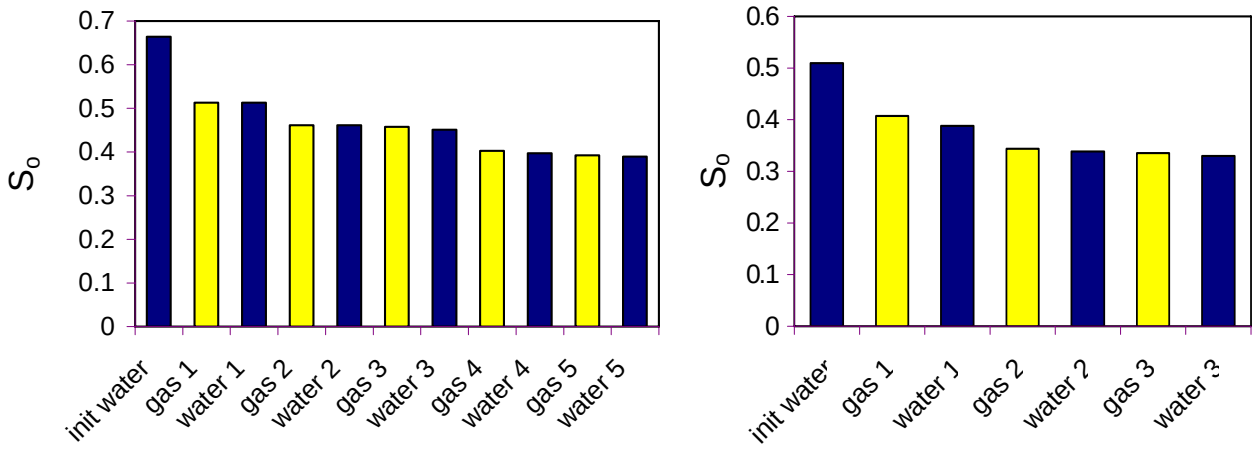

Figure 11 - Residual oil saturations during the simulation of the water-wet (left) and oil-wet (right) micromodel.

In the oil-wet simulation significant recovery was obtained during the WAG operation, but an important difference with the water-wet simulation is that oil production and movement had already ceased after two WAG cycles. Also in the mixed-wet simulation production ceased after two or three WAG cycles.

Comparison of the displacement chain statistics

The displacement statistics for the water-wet simulation are presented in Figure 12 and should be compared with Figure 4 for the base case mixed-wet simulation. Notice that the displacement statistics for the water-wet model start with the first gasflood. An important difference occurs during the first gas flood. Although both cases show significant production during this flood, in the water-wet case this is mainly the result of single and some double displacements, while in the mixed-wet case a significant number of multiple chains are visible. This is also reflected in the type of displacements, as in the water-wet case predominantly (single) g→o displacements have occurred. The latter can be explained by the high oil saturation, making oil continuous throughout the model.

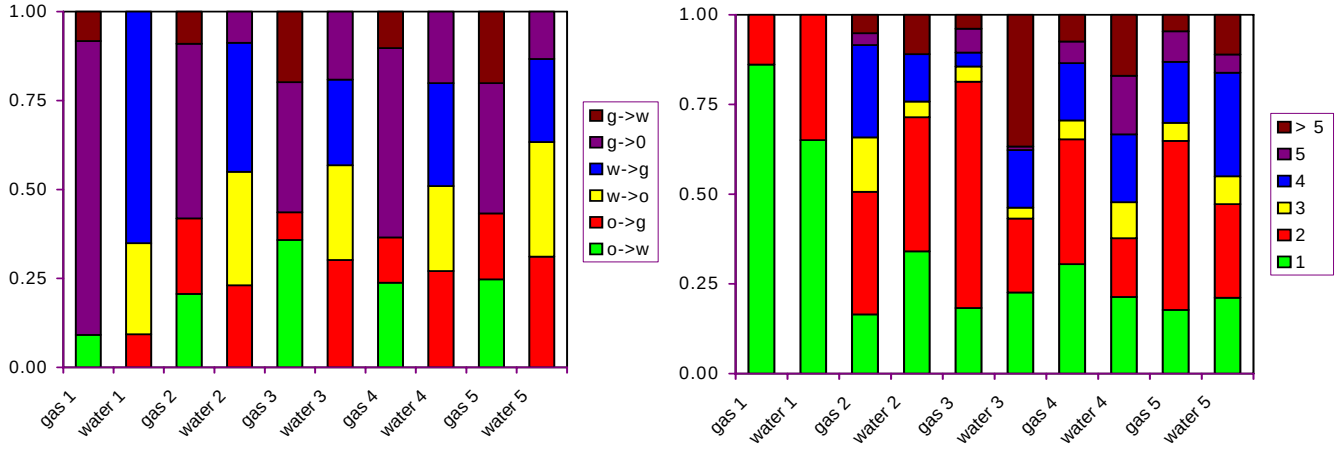

Figure 12 – Types of displacement (left) and displacement chain lengths (right) during consecutive WAG cycles for the water-wet simulation.

During the later WAG cycles, significant numbers of multiple chains also occurred in the water-wet case, although the number of doubles remained much higher than for the mixed-wet case. This can be attributed to the high continuity of water through wetting films in all pores of the model. On the other hand, in the mixed-wet case multiple displacements disappeared during the third and fourth WAG cycles and displacements became dominated by g→w and w→g displacements. This indicates that oil completely ceased to move, contrary to the water-wet case. Another reason is that in the water-wet case oil was the intermediate-wetting phase, such that it was moved from smaller to bigger pores during water floods, by double displacements, and vice versa during gas floods.

The displacement statistics for the oil-wet simulation are presented in Figure 13. Although there are quantitative differences, these statistics are broadly similar to the statistics for the mixed-wet case, presented in Figure 4. The only difference is that in the oil-wet case, oil movement and indeed oil production already ceased after the second WAG cycle, while this happened after the third cycle in the mixed-wet case.

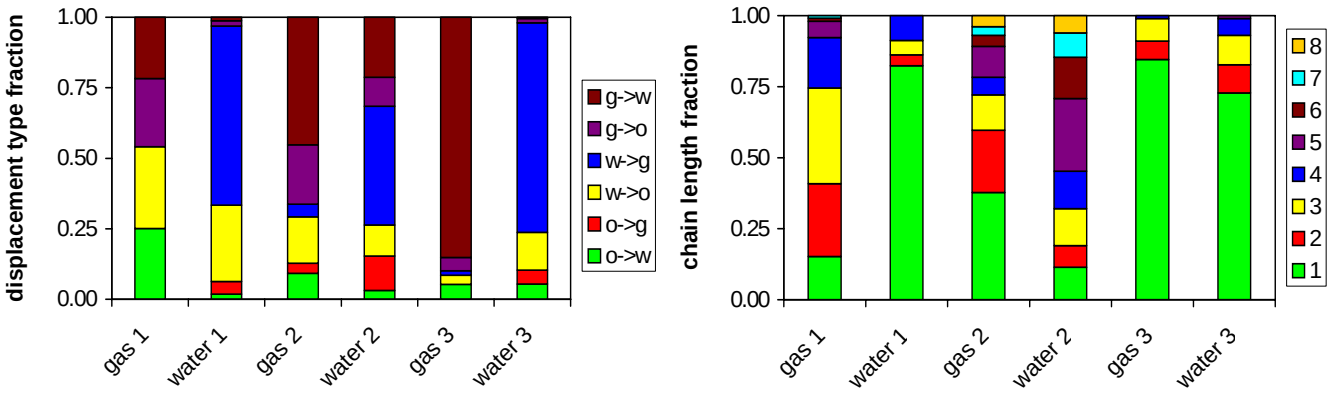

Figure 13 - Types of displacement and displacement chain lengths during consecutive WAG cycles for the oil-wet simulation.

The similarity of the mixed-wet and oil-wet results is surprising, considering the substantial differences between the two cases. For example, in the mixed-wet case water is mainly wetting or intermediate-wetting, but it is the non-wetting phase in the strongly oil-wet case. Furthermore, in the mixed-wet case oil wetting films around gas (in the oil-wet pores) were allowed, compared to oil wetting films around water in a fraction of pores in the oil-wet case. However, the latter could also be the explanation of the similarities, i.e. in both cases the additional oil phase continuity came from films in both cases, contrary to the water-wet case.

Conclusions

Using a 3-D pore-scale network model for three-phase immiscible flow in porous media of arbitrary wettability in 2D mode, previously carried out WAG experiments in mixed-wet micromodels have been simulated. Results from the three experiments, which had slightly different fractions of oil-wet and water-wet pores, were difficult to distinguish. Therefore, in the comparison the three experiments have been considered as “one”. A limited sensitivity study was then carried out with respect to the wettability characteristics, i.e. the contact angle values and distribution, and the fraction of water-wet pores. Based on this study a network model base case has been chosen and the corresponding simulation results have then been compared in detail with the mixed-wet micromodel experimental fluid distributions and displacement statistics. A further comparison has been made between the current modelling of mixed-wet experiments and previous simulations of water-wet and oil-wet experiments

Conclusions are as follows:

(i) The sensitivity study resulted only in small differences between the various cases. Simulations with the largest fraction of water-wet pores tended to have the largest oil residuals. The difference in residuals between cases with different fractions of water-wet pores was larger for cases with contact angles close to 90 degrees. Choosing distributed rather than constant contact angles led to very similar results. These trends were not all unambiguously in agreement with the experimental results.

(ii) For the base case simulation very good qualitative and quantitative agreement between the experimental and simulated recoveries was found. Also the trend along which production ceased during the WAG cycles is similar, as well as some “random jumps” in the recovery profile.

(iii) Displacement statistics obtained from the simulation indicated that many multiple displacements chains occured, also involving movement of oil. The latter ceased after the third WAG cycle in agreement with the recovery trend.

(iv) Detailed comparison of the fluid distributions in experiment and simulation showed generally good agreement: (a) different gas fingers were observed during the various gas floods, (b) oil movement was observed mainly during the first couple of WAG cycles and (c) during water floods, significant amounts of gas were displaced.

(v) Comparison between residual oil saturations and displacement statistics resulting from simulations of the water-wet, oil-wet and mixed-wet micromodel experiments showed large similarities between mixed-wet and oil-wet, as opposed to water-wet. The likely explanation is that in both the mixed-wet and the oil-wet cases oil maintained some additional continuity through wetting films, while in the water-wet case water was continouous through wetting films in all pores.

Acknowledgment

The authors would like to dedicate this paper to their late mentor and colleague, Professor Ali Danesh. He developed the high pressure three-phase micromodel techniques at Heriot-Watt U. and his contribution has been an inspiration. The following members of the Heriot-Watt WAG Consortium are thanked for supporting this research: The UK Department of Trade and Industry, BP, Shell, BHP, Total, Norsk Hydro and Statoil.

References

Dong M., Foraie J., Huang S., and Chatzis I. 2005. Analysis of immiscible water-alternating-gas (WAG) injection using micromodels. *J. Can. Pet. Techn.* **44** (2): 17-25.

Keller A.A., Blunt M.J. and Roberts, A.P.V. 1997: Micromodel observation of the role of oil layers in three-phase flow. *Transport in Porous Media* **26**: 277-297.

Laroche, C. 1998. Secondary and tertiary gas injection experiments in heterogeneous wettability micromodels. SPE 52067, Proc. SPE European Petroleum Conference, The Hague, October 1998.

Laroche, C., Vizika, O., Kalydjian, F. 1999. Network modeling as a tool to predict three-phase gas injection in heterogeneous wettability porous media. *J. Pet. Sci. Eng.* **24**: 155-168.

Øren, P.E., Pinczewski, W.V. 1994. Effect of wettability and spreading on the recovery of waterflood residual oil by immiscible gas flooding. *SPE Formation Evaluation* **9**: 149-156.

Øren, P.E and Pinczewski, W.V. 1995. Fluid distributions and pore-scale displacement mechanisms in drainage dominated three-phase flow. *Transport in Porous Media* **20**: 105-133.

Pereira, G.G., 1999. Numerical pore-scale modelling of three-phase fluid flow: comparison between simulation and experiment. *Phys. Rev. E*. **59**: 4229-4242.

Sohrabi, M., Tehrani, D.H., Danesh, A. and Henderson, G.D. 2001. Visualisation of oil recovery by Water Alternating Gas (WAG) injection using high pressure micromodels – oil-wet system & mixed-wet systems. SPE 71494, Proc. SPE Annual Technical Conference and Exhibition, New Orleans, October 2001.

Sohrabi, M., Tehrani, D.H., Danesh, A. and Henderson, G.D. 2004. Visualization of oil recovery by water-alternating-gas injection using high-pressure micromodels. *SPE J.* **9**: 290-301.

Suicmez, V.S., Piri, M. and Blunt, M.J., 2007. Pore-scale simulation of water alternate gas injection. *Transport in Porous Media* **66**: 259-286.

van Dijke, M.I.J. and Sorbie, K.S. 2002a. Pore-scale network model for three-phase flow in mixed-wet porous media. *Phys. Rev. E.*, **66**: 046302.

van Dijke, M.I.J., Sorbie K.S. 2002b. The relation between interfacial tensions and wettability in three-phase systems: consequences for pore occupancy and relative permeability. *J. Pet. Sci. Eng.* **33**: 39-48.

van Dijke, M.I.J. and Sorbie, K.S. 2003. Pore-scale modelling of three-phase flow in mixed-wet porous media: multiple displacement chains. *J. Pet. Sci. Eng.* **39**: 201-216.

van Dijke, M.I.J., Sorbie, K.S., Sohrabi, M. and Danesh, A. 2004a. Three-phase flow WAG processes in mixed-wet porous media: pore-scale network simulations and comparison with water-wet micromodel experiments, *SPE J.* **9**: 57-66.

van Dijke, M.I.J., Lago, M, Sorbie, K.S. and Araujo, M. 2004b. Free energy balance for three fluid phases in a capillary of arbitrarily shaped cross-section: capillary entry pressures and layers of the intermediate-wetting phase. *J. Colloid Interf. Sci.* **277***:*184-201.

van Dijke, M.I.J., Sorbie, K.S., Sohrabi, M. and Danesh, A. 2006. Simulation of WAG floods in an oil-wet micromodel using a 2-D pore scale network model. *J. Pet. Sci. Eng.* **52**: 71-86.

Vizika, O., Lombard, J.-M. 1996. Wettability and spreading: two key parameters in oil recovery with three-phase gravity drainage. *SPE Reservoir Engineering* **11**: 54-60.